Anchor Structure of Cell Wall Surface Proteins in *Listeria monocytogenes*†

Gautam Dhar,‡ Kym F. Faull,§ and Olaf Schneewind*,‡

Departments of Microbiology and Immunology and of Psychiatry and Biobehavioral Sciences, University of California Los Angeles School of Medicine, Los Angeles, California 90095

Received October 8, 1999; Revised Manuscript Received January 13, 2000

ABSTRACT: Many surface proteins of Gram-positive bacteria are anchored to the cell wall by a mechanism requiring a COOH-terminal sorting signal with a conserved LPXTG motif. In *Staphylococcus aureus*, surface proteins are cleaved between the threonine and the glycine of the LPXTG motif. The carboxyl of threonine is subsequently amide linked to the amino group of the pentaglycine cell wall crossbridge. Here we investigated the anchor structure of surface proteins in *Listeria monocytogenes*. A methionine and six histidines (MH_6) were inserted upstream of the LPXTG motif of internalin A (InlA), a cell-wall-anchored surface protein of *L. monocytogenes*. The engineered protein InlA-MH_6-Cws was found anchored in the bacterial cell wall. After peptidoglycan digestion with phage endolysin, InlA-MH_6-Cws was purified by affinity chromatography. COOH-terminal peptides of InlA-MH_6-Cws were obtained by cyanogen bromide cleavage followed by purification on a nickel−nitriloacetic acid column. Analysis of COOH-terminal peptides with Edman degradation and mass spectrometry revealed an amide linkage between the threonine of the cleaved LPXTG motif and the amino group of the *m*-diaminopimelic acid crossbridge within the listerial peptidoglycan. These results reveal that the cell wall anchoring of surface proteins in Gram-positive bacteria such as *S. aureus* and *L. monocytogenes* occurs by a universal mechanism.

Gram-positive bacteria display proteins on their surface as a means to interact with host tissues and to establish human infections *(1)*. Studies on staphylococcal protein A revealed that the anchoring of surface protein to the cell wall requires a NH_2-terminal leader (signal) peptide and a 35 residue COOH-terminal sorting signal *(2−4)*. The sorting signal includes a conserved LPXTG motif followed by a hydrophobic domain and a tail of mostly positively charged residues *(3)*. After synthesis in the bacterial cytoplasm, surface protein precursors are translocated across the membrane and the NH_2-terminal leader peptide is removed by leader peptidase *(5)*. The COOH-terminal sorting signal functions first to retain the polypeptide from the secretory pathway *(2, 3)*. Retention is followed by cleavage between the threonine and the glycine of the LPXTG motif *(5)* and then by amide linkage of the carboxyl of threonine to the pentaglycine crossbridge of the staphylococcal cell wall *(6−9)*. This cell wall sorting reaction is catalyzed by a small membrane protein named sortase *(10)*.

Antibiotic inhibition of peptidoglycan precursor (lipid II) incorporation into cell wall also inhibits surface protein anchoring *(11)*, suggesting that the membrane-tethered lipid II may serve as the peptidoglycan substrate of the sorting reaction *(12, 13)*. Surface protein linked to peptidoglycan precursor may subsequently be incorporated into the cell wall via the transglycosylation and transpeptidation reactions *(13)*. The addition of strong nucleophiles such as hydroxylamine causes the release of surface protein hydroxamate from staphylococci, suggesting that polypeptides which have been cleaved at the LPXTG motif form an acyl enzyme intermediate with sortase *(14)*. During cell wall anchoring, the acyl enzyme intermediate between surface protein and sortase is thought to be resolved by the nucleophilic attack of the free amino of the peptidoglycan crossbridge.

An LPXTG motif has been found within sorting signals of more than 100 surface proteins *(1)*. Amino groups of cell wall crossbridges are also a conserved feature of bacterial peptidoglycans *(15)*, suggesting that the cell wall sorting mechanism of *S. aureus* may be universal in Gram-positive bacteria. This hypothesis is supported by the conservation of the sortase gene in Gram-positive bacteria *(10)* and by the observation that heterologous sorting signals can anchor surface proteins when expressed in *S. aureus (3)*. Nevertheless, the universality of the sorting reaction has never been rigorously tested. Here we examined cell wall anchoring of surface proteins in *Listeria monocytogenes*, an organism that was chosen because its peptidoglycan crossbridge (*m*-Dpm)[1] is chemically distinct and much shorter than the pentaglycine crossbridge of staphylococci *(15−17)*. By using a combina-

† This work was supported by the U.S. Public Health Service, Grant AI 38897 (Infectious Diseases Branch, National Institute of Allergy and Infectious Diseases, National Institutes of Health). K.F.F. was supported by a grant from the Keck Foundation.

* To whom correspondence should be addressed: Department of Microbiology and Immunology, UCLA School of Medicine, 10833 Le Conte Ave., Los Angeles, CA 90095. Tel. (310) 206-0997; Fax (310) 267-0173; E-mail olafs@ucla.edu.

‡ Department of Microbiology and Immunology.

§ Department of Psychiatry and Biobehavioral Sciences.

[1] Abbreviations: BHI, brain heart infusion; CID, collisionally induced dissociation; CNBr, cyanogen bromide; Cws, cell wall sorting signal; *m*-Dpm, *m*-diaminopimelic acid; ESI-MS, electrospray ionization mass spectrometry; MALDI-MS, matrix-assisted laser desorption ionization mass spectrometry; MS/MS, tandem mass spectrometry; *m*/*z*, mass-to-charge ratio; PPG, poly(propylene glycol); rpHPLC, reverse-phase high-performance liquid chromatography; InlA, internalin A; TFA, trifluoroacetic acid.

10.1021/bi992347o CCC: $19.00
Published on Web 03/08/2000

tion of molecular biology and mass spectrometry, we now demonstrate that surface proteins of *L. monocytogenes* are cleaved between the threonine and the glycine of the LPXTG motif. The carboxyl of threonine is amide-linked to the amino of *m*-Dpm, thereby revealing the universality of the cell wall sorting mechanism.

EXPERIMENTAL PROCEDURES

Bacterial Strains and Plasmids. To express the hybrid protein InlA-MH_6-Cws, the coding sequence for the InlA sorting signal harboring the engineered methionine−histidine affinity tag was PCR-amplified from the chromosomal DNA of *L. monocytogenes* EGD with the primers InlA2 (AAGGATCCACATCTAGCTCTTTACACTA) and InlA4 (AAGGTACCATGCATCACCATCACCATCACGAAGCTTCACTCCCTACAACT). The PCR product was digested with *Kpn*I and *Bam*HI and cloned into the corresponding sites of pOS2 to generate pGD13. DNA specifying InlA promoter and upstream sequences were amplified with primers InlA6 (AAGGTACCGGAGTGACATGCTTTTTAACAA) and InlA7(AAGGTACCATTATAAGGGTCATAAGCGTTCA), digested with *Kpn*I, and then cloned into the corresponding site of pGD13 to generate pGD21.The MH_6 tag of InlA-MH_6-Cws replaces the amino acids SK at position 726 of mature internalin.

Transformation of L. monocytogenes. Overnight cultures of *L. monocytogenes* strain EGD were diluted 1:20 into 300 mL of BHI containing 0.5 M sucrose and incubated at 37 °C with shaking until OD_{600} 0.4. Penicillin G was added to a final concentration of 12.5 μg/mL and cultures were incubated for 2 h (OD_{600} approximately 0.8). Cells were harvested by centrifugation at 4 °C, washed with 0.5 M sucrose, and suspended in 500 μL of 0.5 M sucrose. Penicillin protoplasts were stored at −80 °C in aliquots of 100 μL. For transformation, 50 μL competent cells were thawed at 4 °C, mixed with 1 μg of dialyzed plasmid DNA, and electroporated in a 0.2 cm cuvette at 200 Ω resistance, 25 μF capacitance, and 2 kV. Cells were immediately diluted with 1 mL of BHI containing 0.5 M sucrose, allowed to incubate at 37 °C for 1 h, and plated on BHI-agar plates containing 5 μg/mL erythromycin. Colonies appeared after 4−5 days. Plasmids were purified from *Listeria* using the Qiagen miniprep kit according to the manufacturer's recommendations.

Protein Topology Assays. L. monocytogenes EGD and EGD(pGD21) were grown overnight in BHI without or with 5 μg/mL erythromycin, diluted 1:20 into the same medium and grown until OD_{600} 0.6−0.7. One milliliter of culture was centrifuged at 15000*g* for 5 min, and cells were washed and suspended in 1 mL of minimal medium 4 *(2)*. Proteins were pulse-labeled by the addition of 30 μCi of [^{35}S]methionine for 1 min and all further incorporation of radioactive amino acid was quenched by adding 50 μL of chase solution (containing per milliliter 100 mg of casamino acids, 20 mg of methionine, 20 mg of cysteine, 4 mg of chloramphenicol, and 20 μL of mercaptoethanol).

To determine the solubility of surface proteins in hot SDS, two 0.5 mL aliquots of pulse-labeled *Listeria* culture were precipitated with 5% ice-cold trichloroacetic acid and the sediment was washed in acetone and dried. One sample was suspended in 0.5 M Tris-HCl, pH 8.0, and the peptidoglycan was digested with 100 units of endolysin at 37 °C for 30 min (monitored as a descrease in absorption at OD_{600}). The digested sample was again precipitated with trichloroacetic acid. Both endolysin-digested and undigested samples were suspended in 55 μL of 4% SDS and 0.5 M Tris-HCl, pH 8.0, and boiled in a heated water bath for 10 min. Samples were centrifuged at 15000*g* for 5 min and 45 μL of soluble supernatant was subjected to immunoprecipitation.

For cell fractionation, 1 mL aliquots of pulse-labeled *Listeria* culture were incubated for 20 min after the addition of chase solution. Cells were sedimented by centrifugation at 15000*g* for 5 min and the supernatant, representing the extracellular medium, was precipitated with 5% ice-cold trichloroacetic acid. Cells were suspended in 1 mL of SMM buffer (50 mM Tris-HCl, 100 mM NaCl, 500 mM sucrose, and 10 mM $MgCl_2$, pH 8.0) and peptidoglycan was digested with 100 units of endolysin for 10 min at 37 °C. After centrifugation at 15000*g* for 5 min, the supernatant containing the digested cell wall compartment was separated from the protoplast sediment and precipitated with trichloroacetic acid. Protoplasts were suspended in 1 mL of 50 mM Tris-HCl and 150 mM NaCl, pH 7.5, and lysed by repeated freeze/thawing in a dry ice−ethanol bath, and membranes were sedimented by centrifugation at 100000*g* for 30 min. The supernatant containing *Listeria* cytosol was separated from the membrane pellet, which was suspended in 1 mL of 50 mM Tris-HCl and 150 mM NaCl, pH 7.5. All samples were precipitated with 5% ice-cold trichloroacetic acid, washed in acetone, and dried. Pellets were suspended in 55 μL of 4% SDS and 0.5 M Tris-HCl, pH 8.0, boiled in a heated water bath for 10 min, and centrifuged to remove insoluble material.

For immunoprecipitation, 45 μL of pulse-labeled sample was added to 1 mL of RIPA buffer (50 mM Tris-HCl, 150 mM NaCl, 1% Triton X-100, 0.5% deoxycholate, and 0.1% SDS, pH 8.0) containing 1:1000 diluted rabbit antiserum and incubated with shaking at room temperature for 1 h. Protein A−Sepharose, 50 μL of a 50% slurry of beads preswollen in 50 mM Tris-HCl, 150 mM NaCl, and 10 mM EDTA, pH 7.5, was added and immune complexes were collected by shaking at room temperature for 1 h followed by centrifugation at 4000*g* for 2 min and five washes with RIPA buffer. The beads were suspended in 20 μL of sample buffer and boiled for 10 min to release immunoprecipitated species, which were then separated on SDS−PAGE and analyzed by PhosphorImager.

Purification of InlA-MH_6-Cws. L. monocytogenes EGD-(pGD21) and EGD were grown in BHI with or without 5 μg/mL erythromycin at 37 °C to OD_{600} 1.0. Cells were sedimented by centrifugation at 8000*g* for 30 min, washed with 500 mL of ice-cold water, and suspended in 100 mL of water. Bacterial carbohydrates were extracted by the addition of 100 mL of an ethanol−acetone (1:1) mixture and incubation for 30 min on ice. The cells were washed with 300 mL of ice-cold water, suspended in 30 mL of SMM buffer, and digested with 1500 units of endolysin for 12−14 h at 37 °C. Endolysin-released surface proteins were separated from the protoplasts by centrifugation at 8000*g* for 30 min. Supernatant containing endolysin-released InlA-MH_6-Cws surface protein was purified by affinity chromatography on Ni−NTA−Sepharose (Qiagen). A column with 1.2 mL of bed volume was washed with 15 mL of

equilibration buffer (EB; 50 mM Tris-HCl and 150 mM NaCl, pH 7.5), loaded with 30 mL of cell wall extract, washed first with 30 mL of EB and then with 30 mL of wash buffer (WB; 50 mM Tris-HCl, 150 mM NaCl, 10% glycerol, and 10 mM imidazole, pH 7.5). Bound protein was eluted with 5 mL of elution buffer (ELB; 0.5 M imidazole, 50 mM Tris-HCl, 150 mM NaCl, and 10% glycerol, pH 7.5) and 1 mL fractions were collected.

Purification of InlA-MH_6-Cws from Isolated Cell Walls. *L. monocytogenes* EGD(pGD21) was grown in 6 L of BHI containing erythromycin at 37 °C to OD_{600} 1.0. Cells were sedimented at 8000*g* for 30 min, washed with 500 mL of 50 mM Tris-HCl buffer, pH 7.5, and suspended in 50 mL of the same buffer supplemented with 1 μM pepstatin and 1 mM PMSF. *Listeria* were broken in a Bead-Beater instrument (Biospec Products, Bartlesville, OK) with 15 pulses of 40 s each follwed by 5 min of incubation on ice (*9*). The lysate was cleared from glass beads by centrifugation at 1000*g* for 5 min. The cell lysate was removed with the supernatant and murein sacculi were sedimented by centrifugation at 20000*g* for 20 min. Cell walls were suspended in 50 mL of wash buffer (100 mM potassium phosphate, pH 7.5, 1% Triton X-100, 1 μM pepstatin, and 1 mM PMSF), stirred for about 45 min at 4 °C to dissolve contaminating membranes, and centrifuged at 40000*g* for 30 min. Cell walls were washed three times with 100 mM sodium phosphate buffer, pH 8.0, suspended in 100 mM Tris-HCl and 150 mM NaCl, pH 8.0, and incubated at 37 °C for 16 h with 1500 units of endolysin. Unigested cell walls were removed by centrifugation at 5000*g* and the supernatant was loaded on a 1.2 mL Ni−NTA−Sepharose column as described above.

Purification of Endolysin. Bacteriophage endolysin was expressed in *E. coli* and affinity-purified via an appended affinity tag as described by Loessner et al. *(18)*. Briefly, *Escherichia coli* JM109(pHLP118) was grown in 2 L of Luria broth at 37 °C to OD_{600} 0.7, induced with 1 mM IPTG, and grown to OD_{600} 1.0. Cells were harvested at 6000*g* for 15 min, washed, and suspended in 30 mL of buffer F (50 mM Tris-HCl, pH 7.5, 20% sucrose, 500 mM NaCl, and 5 mM imidazole). *E. coli* cells were broken by two passages through a French pressure cell at 14 000 psi. The lysate was centrifuged three times at 15000*g* for 15 min and the supernatant was loaded onto a 2.5-mL Ni−NTA column preequilibrated with 30 mL of EB, washed with 30 mL of WB, and finally eluted with 10 mL of ELB. The enzyme was assayed for activity with heat-killed *listeria* cells as a crude peptidoglycan substrate. One unit of activity is defined as the amount of endolysin necessary to decrease the OD_{600} by 0.01/min in 50 mM Tris-HCl, pH 8.0, at 25 °C in a volume of 1 mL with heat-killed, washed *L. monocytogenes* EGD as substrate.

Cyanogen Bromide Cleavage of InlA-MH_6-Cws. Affinity-purified InlA-MH_6-Cws was precipitated with methanol−chloroform and dissolved in 150 μL of 70% formic acid. CNBr was added to saturation and the reaction mixture was incubated for 36 h at room temperature. Cleaved peptides were dried under vacuum, suspended twice in 100 μL of water, dried to remove excess CNBr, and suspended in 1 mL of buffer A (6 M guanidine hydrochloride, 0.1 M NaH_2PO_4, and 0.01 M Tris-HCl, pH 8.0). A 1.2 mL column of Ni−NTA−Sepharose was preequilibrated with 10 mL of buffer A and loaded with the CNBr-cleaved peptides. The column was washed successively with 10 mL of buffer A, 10 mL of buffer B (8 M urea, 0.1 M NaH_2PO_4, and 0.01 M Tris-HCl, pH 8.0), and 10 mL of buffer C (same as buffer B, but pH 6.3). The anchor peptides were finally eluted with a mixture of 2 mL of buffer E (same as buffer B but pH 4.5 and 1 mL of 0.5 M acetic acid. The eluate was desalted on a 2-mL C18 cartridge *(7)*.

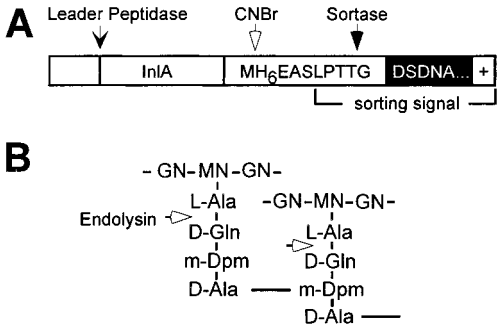

FIGURE 1: Structure of InlA-MH_6-Cws surface protein and of the cell wall of *L. monocytogenes*. (A) Structure of recombinant surface protein (InlA-MH_6-Cws) harboring an NH_2-terminal signal (leader) peptide with leader peptidase cleavage site as well as a COOH-terminal cell wall sorting signal consisting of an LPXTG motif, followed by a hydrophobic domain (shaded box) and positively charged tail (boxed +). Upstream of the LPXTG motif, a methionine followed by a six histidine tag was inserted that allowed purification of the recombinant InlA-MH_6-Cws on Ni−NTA and cleavage at methionine with cyanogen bromide (CNBr). (B) Structure of the listerial peptidoglycan illustrating the cleavage sites of phage endolysin (open arrow) *(26)*. The abbreviations GN (GlcNac) and MN (MurNac) were used for the amino sugars within the glycan chains.

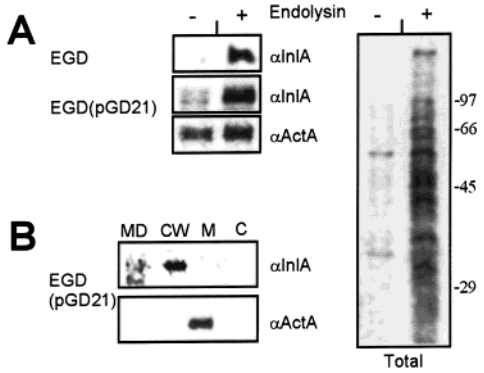

FIGURE 2: Anchoring of InlA-MH_6-Cws to the cell wall of *L. monocytogenes*. (A) To measure protein linkage to the cell wall, the peptidoglycan of pulse-labeled listeria was either digested with endolysin (+) or left untreated (−) and trichloroacetic acid-precipitated samples were extracted by boiling in SDS. *L. monocytogenes* wild-type strain EGD expresses internalin (InlA), whereas strain EGD(pGD21) expresses InlA and InlA-MH_6-Cws. Total sample and immunoprecipitated surface protein (α-InlA and α-Act) were analyzed by SDS−PAGE and PhosphorImager, revealing that cell-wall-anchored InlA and InlA-MH_6-Cws were largely insoluble in hot SDS unless the peptidoglycan had first been digested with endolysin. In contrast, the membrane-anchored surface protein ActA was extractable with hot SDS without the need for prior endolysin treatment *(24, 25)*. (B) Pulse-labeled *L. monocytogenes* EGD-(pGD21) cultures were fractionated into culture medium (MD), cell wall (CW), membrane (M), and cytosolic (C) compartments. Surface proteins were immunoprecipitated and analyzed by SDS−PAGE and PhosphorImager. InlA and InlA-MH_6-Cws are anchored to the cell wall compartment, whereas ActA is located in the membrane.

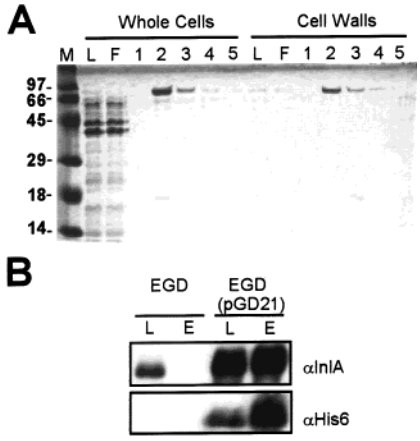

FIGURE 3: Purification of InlA-MH_6-Cws from endolysin digested listeria or from isolated listerial cell walls. (A) Coomassie-stained SDS−12% PAGE of affinity-purified (Ni−NTA) InlA-MH_6-Cws: load (L) and flowthrough (F) as well as five 1 mL eluate fractions (1−5). *L. monocytogenes* EGD(pGD21) was digested with endolysin and protoplasts were sedimented by centrifugation. The cell wall lysate in the supernatant was subjected to affinity chromatography (whole cells). In another experiment, the murein sacculi of strain EGD(pGD21) were isolated and digested with endolysin prior to affinity chromatography (cell walls). (B) Immunoblotting analysis of load (L) and eluate (E) fractions after Ni−NTA affinity purification of endolysin-digested *L. monocytogenes* EGD or EGD-(pGD21) using α-InlA and hexahistidine probe (6-His, Pierce). InlA-MH_6-Cws, but not wild-type InlA, was bound and purified on Ni−NTA−Sepharose.

rpHPLC of Anchor Peptides. C18 cartridge-desalted peptides were dried and dissolved in 200 μL of 0.1% TFA, filtered, and then subjected to rpHPLC on C18 column (2 × 250 mm Betasil, Keystone Scientific). Separation was carried out at room temperature with a linear gradient from 5% CH_3CN (in H_2O, 0.1% TFA) to 100% CH_3CN (0.1% TFA) in 95 min at a flow rate of 0.2 mL/min. The elution of anchor peptides was monitored at 214 nm, and fractions were collected at 1 mL/min. Collected fractions were dried under vacuum and suspended in CH_3CN−water−formic acid (50:50:0.1) for mass spectrometry analysis.

MALDI-MS. MALDI-MS spectra were obtained on a reflectron time-of-flight instrument (PerSeptive Biosystems Voyager RP) in the linear mode *(7)*. Samples (0.5 μL) were cospotted with 0.5 μL of matrix [α-cyano-4-hydroxycinnamic acid, 10 mg/mL in CH_3CN−water−TFA (70:30:0.1)]. All samples were externally calibrated to a standard of bovine insulin.

ESI-MS of Anchor Peptides. Dried muropeptides were dissolved in 40 μL of water−CH_3CN−formic acid (50:50:0.1). A Perkin-Elmer Sciex API III triple-quadrupole mass spectrometer was tuned and calibrated as previously described *(7)*. Samples were introduced into the ionization source by flow injection. ESI-MS and MS/MS spectra were obtained by degraded mass resolution to improve sensitivity of detection. Step sizes of 0.3 and 1.0 Da were used for the recording of MS and MS/MS spectra, respectively. Under these conditions, the isotopes of the PPG/NH_4^+ singly charged ion at *m*/*z* 906 were not resolved from one another.

RESULTS

Expression and Cell Wall Anchoring of InlA-MH_6-Cws. To purify and characterize COOH-terminal peptides of surface proteins that may be linked to peptidoglycan, we followed a previously established strategy *(7)*. Internalin A is a cell wall-anchored surface protein of *L. monocytogenes* that harbors an NH_2-terminal leader peptide and a COOH-terminal sorting signal *(19−21)*. Internalin A was modified by inserting a methionine and six-histidine tag (MH_6) three amino acids upstream of the COOH-terminal sorting signal to generate InlA-MH_6-Cws (Figure 1). The open reading frame specifying InlA-MH_6-Cws was cloned into an *E. coli*−*Listeria* shuttle plasmid to generate pGD21, which was transformed into *L. monocytogenes* strain EGD (*22*). InlA-MH_6-Cws was expressed from the internalin (*inlA*) promoter *(23)*.

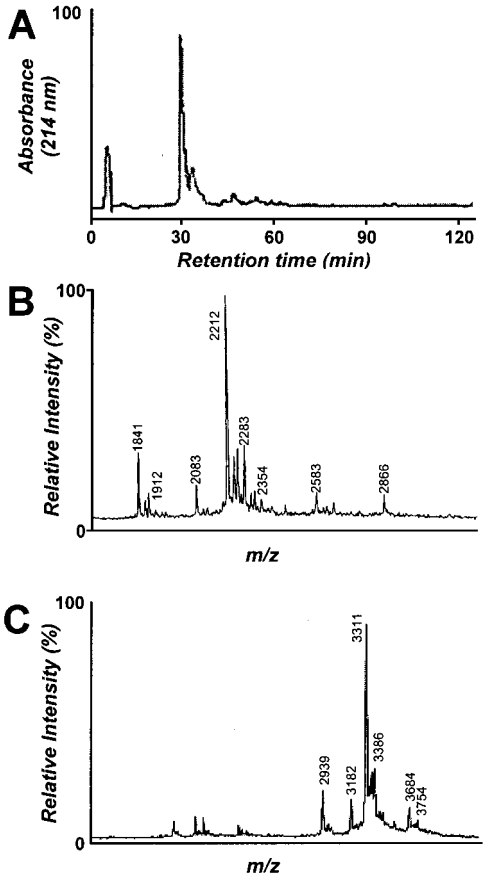

FIGURE 4: Characterization of endolysin-solubilized COOH-terminal anchor peptides of InlA-MH_6-Cws. (A) rpHPLC of CNBr-cleaved and affinity-purified InlA-MH_6-Cws peptides. Endolysin-solubilized InlA-MH_6-Cws was purified by affinity chromatography and cleaved with CNBr, and the COOH-terminal anchor peptides were isolated by affinity chromatography on Ni−NTA. The sample was desalted over a C18 cartridge and subjected to rpHPLC. (B) MALDI-MS of the eluted fraction at 25% CH_3CN. Numbers indicate the *m*/*z* values of the identified ions. See Table 2 for a complete listing of the observed ions, proposed structures and calculated masses. (C) MALDI-MS of the eluted fraction at 28% CH_3CN. Numbers indicate the *m*/*z* values of the identified ions. See Table 3 for a complete listing of the observed ions, proposed structures, and calculated masses.

Cell wall sorting of InlA-MH_6-Cws was measured in two ways. First, listeria were grown in minimal medium and pulse-labeled with [^{35}S]methionine. Twenty minutes after the addition of the chase, the culture was divided into two aliquots, each of which was precipitated with trichloroacetic acid. One sample was directly boiled in SDS, whereas the other was first treated with phage endolysin to digest the bacterial cell wall and then boiled in SDS (Figure 2). Wild-

Table 1: Edman Degradation of COOH-Terminal Anchor Peptides of InlA-MH_6-Cws

cycle	residue	concn[a] (pM)	cycle	residue	concn[a] (pM)
1	His (Ala)	194 (64)[b]	8	Ala	78
2	His	291	9	Ser	20
3	His	280	10	Leu	41
4	His	331	11	Pro	0[c]
5	His	293	12	Thr	18
6	His	272	13	Thr	35
7	Glu	58			

[a] Aliquots of rpHPLC-purified anchor peptides were analyzed by MALDI-MS and Edman degradation. The picomolar concentration of observed phenylthiohydantoin-coupled amino acid peaks per Edman cycle is reported. [b] During cycle 1, the sample yielded two phenylhydantoin-coupled amino acids (histidine and alanine). [c] This sequenator run did not permit detection of phenylthiohydantoin-proline.

Table 2: Structures of Anchor Peptides Identified in rpHPLC Fraction 30

observed *m/z*[a]	calculated *m/z*[b]	Δobs−calc[c]	proposed structure[d]
1841.1	1841.9	−0.8	D-iGln-*m*-Dpm-(A)
1911.7	1913.0	−1.3	D-iGln-m-Dpm-(A)-D-Ala
2083.2	2085.2	−2.0	X-(A)-*m*-Dpm
2212.3	2213.3	−1.0	X-(A)-*m*-Dpm-(D-iGln)
2283.4	2284.4	−1.0	X-(A)-X
2354.5	2355.5	−1.0	X-(A)-Y/Y-(A)-X
2583.0	2584.8	−1.8	X-(A)-X-*m*-Dpm-D-iGln
2866.0	2869.1	−3.1	Y-(A)-Y-Y

[a] Affinity chromatography- and rpHPLC- (fraction 30, 25% CH_3CN) purified anchor peptides were analyzed by MALDI-MS. The *m/z* of observed ions is compared with the *m/z* of proposed anchor peptide structures. [b] Calculations are for singly protonated species $[M + H]^+$. [c] The difference between the observed and calculated molecular mass is in agreement with the expected error rate (0.1%) for this type of measurement. [d] A = H_2N-H_6EASLPTT; X = D-iGln-m-Dpm-D-Ala; Y = L-Ala-D-iGln-*m*-Dpm-D-Ala.

type InlA of strain EGD was insoluble in hot SDS unless the listerial peptidoglycan was digested with endolysin (Figure 2A). Transformation of strain EGD with the high-copy-number plasmid pGD21 caused a 5−7-fold increase in the amount of radiolabeled internalin, suggesting that InlA-MH_6-Cws (encoded by pGD21) was expressed at much higher levels than wild-type InlA. Less than 20% internalin of strain EGD(pGD21) was directly soluble in hot SDS, suggesting that both InlA and InlA-MH_6-Cws were anchored to the bacterial cell wall (Figure 2A). As a control, more than 80% of the membrane-anchored surface protein ActA was soluble in hot SDS even without endolysin digestion of the bacterial cell wall *(24, 25)*.

As a second measure for the cell wall anchoring of InlA and InlA-MH_6-Cws, the location of internalin was examined in pulse-labeled EGD(pGD21) cultures that were fractionated into the medium, cell wall, cytoplasm, and membrane compartments (Figure 2B). Internalin (InlA and InlA-MH_6-Cws) was located in the cell wall compartment, whereas ActA fractionated with the membranes. Together these data confirmed previous observations that internalin is anchored to the cell wall compartment of *L. monocytogenes (21)*. Furthermore, insertion of the MH_6 tag upstream of the InlA sorting signal does not appear to interfere with the cell wall anchoring of InlA-MH_6-Cws.

Purification of InlA-MH_6-Cws from Listerial Protoplasts and Isolated Cell Walls. Purification of InlA-MH_6-Cws was

Table 3: Structures of Anchor Peptides Identified in rpHPLC Fraction 33

observed *m/z*[a]	calculated *m/z*[b]	Δobs-calc[c]	proposed structure[d]
2939.4	2940.2	−0.8	Y_3-(A)-Ala
3182.0	3183.4	−1.4	Y_3-(A)-Ala-*m*-Dpm-Ala
3310.8	3311.6	−0.8	Y_4-(A)/Y_3X-(A)-Ala
3386.0	3382.6	+3.4	Y_4-(A)-Ala
3684.0	3683.0	−1.0	Y_4X-(A)
3754.3	3754.1	−0.2	Y_5-(A)

[a] Affinity chromatography- and rpHPLC- (fraction 33, 28% CH_3CN) purified anchor peptides were analyzed by MALDI-MS. The *m/z* of observed ions is compared with the *m/z* of proposed anchor peptide structures. [b] Calculations are for singly protonated species $[M + H]^+$. [c] The difference between the observed and calculated molecular mass is in agreement with the expected error rate (0.1%) for this type of measurement. [d] A = H_2N−H6EASLPTT; X = D-iGln-*m*-Dpm-D-Ala. Y = L-Ala-D-iGln-*m*-Dpm-D-Ala.

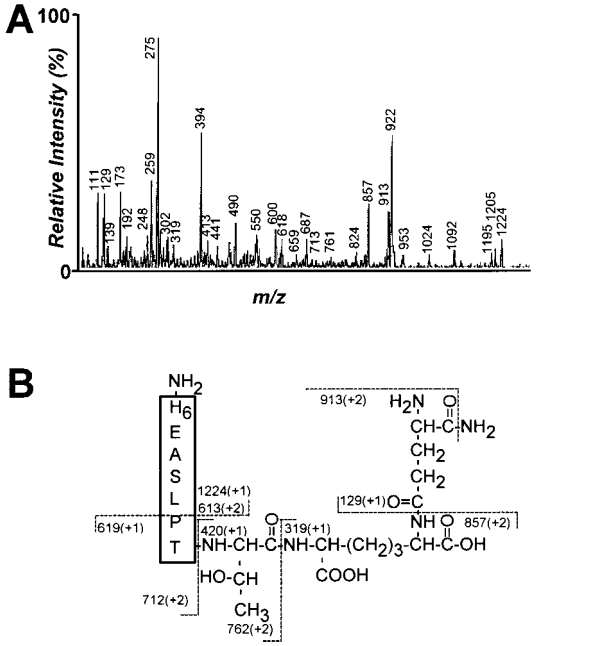

FIGURE 5: Structure of the 1841 Da COOH-terminal InlA-MH_6-Cws anchor peptide from endolysin digested *L. monocytogenes*. (A) MS/MS analysis of the doubly charged parent ion at *m/z* 921.5. (B) CID-generated daughter ions were compared with the structural model. See Table 4 for a complete listing of the observed ions, proposed structures, and calculated masses.

achieved by using two dfferent experimental schemes. First, listeria were digested with phage endolysin in a buffer that osmotically stabilized the resulting protoplasts. Protoplasts were sedimented by centrifugation and the supernatant, containing digested cell wall, was subjected to affinity chromatography on Ni−NTA (whole cells). Coomassie-stained SDS−PAGE of load (L), flowthrough (F), and eluate fractions revealed purification of InlA-MH_6-Cws (Figure 3A). In the second approach, listeria were disrupted by mechanical force using glass beads in a bead-beater instrument. Glass beads were removed by slow-speed centrifugation. The murein sacculi were sedimented from the lysate by high-speed centrifugation, and contaminating membranes were extracted with Triton X-100. Murein sacculi were treated with endolysin and the cell wall digest was subjected to affinity chromatography (cell walls). Coomassie-stained SDS−PAGE revealed purification of InlA-MH_6-Cws from

Table 4: Summary of CID Daughter Ions Produced during MS/MS of the Endolysin-Released Anchor Peptide with *m/z* 1841 and Their Proposed Structural Assignments (Figure 4)

observed *m/z*[a]	charge state	calculated *m/z*[b]	Δobs−calc[c]	proposed structure	ion type[d]
110.9	+1	110.1	+0.8	H	a_1
138.5	+1	138.1	+0.4	H	b_1
70.1	+2	69.6	+0.5	H	b_1
247.7	+1	247.3	+0.4	HH	a_2
258.8	+1	257.3	+1.5	HH(−H_2O)	b_2
275.3	+1	275.3	0.0	HH	b_2
138.5	+2	138.1	+0.4	HH	b_2
413.0	+1	412.4	+0.6	HHH	b_3
394.4	+1	394.4	0.0	HHH (−H_2O)	b_3
549.8	+1	549.6	+0.2	HHHH	b_4
282.5	+2	282.8	−0.3	HHHH	c_4
275.3	+2	275.3	0.0	HHHH	b_4
686.6	+1	686.7	−0.1	HHHHH	b_5
823.7	+1	823.8	−0.1	HHHHHH	b_6
413.0	+2	412.4	+0.6	HHHHHH	b_6
926.3	+1	925.0	+1.3	H_6E	a_7
953.0	+1	953.0	0.0	H_6E	b_7
489.8	+2	489.5	+0.3	H_6EA (−H_2O)	a_8
1024.1	+1	1024.0	+0.1	H_6EA	b_8
513.5	+2	512.5	+1.0	H_6EA	b_8
1092.2	+1	1093.1	−0.9	H_6EAS (−H_2O)	b_9
1111.1	+1	1111.1	0.0	H_6EAS	b_9
555.8	+2	556.1	−0.3	H_6EAS	b_9
1195.1	+1	1196.3	−1.2	H_6EASL	a_{10}
1223.6	+1	1224.3	−0.7	H_6EASL	b_{10}
1205.3	+1	1206.3	−1.0	H_6EASL (−H_2O)	b_{10}
612.5	+2	612.6	−0.1	H_6EASL	b_{10}
599.9	+2	598.6	+1.3	H_6EASL	a_{10}
440.9	+2	441.5	−0.6	HHHEASLP	a_{11}, y_{11}
659.3	+2	661.2	−1.9	H_6EASLP	b_{11}
713.0	+2	711.8	+1.2	H_6EASLPT	b_{12}
761.0	+2	762.3	−1.3	H_6EASLPTT/A[e]	b_{13}
857.0	+2	857.4	−0.4	*m*-Dpm-(A)	$y_{1'}$
902.9	+2	904.4	−1.5	D-iGln-*m*-Dpm-(A)(−NH_2, −H_2O)	
912.5	+2	913.0	−0.5	D-iGln-*m*-Dpm-(A)(−NH_2)	
128.6	+2	129.1	−0.5	D-iGln	$b_{1'}$
173.3	+1	173.2	+0.1	*m*-Dpm (−H_2O)	y_1, $y_{1'}$
191.6	+1	191.2	+0.4	*m*-Dpm	y_1, $y_{1'}$
301.7	+1	301.3	+0.4	*m*-Dpm-(D-iGln) (−H_2O)	y_1
318.8	+1	319.3	−0.5	*m*-Dpm-(D-iGln)	y_1
420.8	+1	420.4	+0.4	T-*m*-Dpm-(D-iGln)	y_2
521.6	+1	521.5	+0.1	T−T-*m*-Dpm-(D-iGln)	y_3
618.2	+1	618.6	−0.4	P−T-T-*m*-Dpm-(D-iGln)	y_4
921.5	+2	921.5	0.0	D-iGln-*m*-Dpm-(A)	parent ion

[a] See Figure 4A for relative intensity of daughter ions. [b] Calculations are based on average masses; for *n* protonated species the formula is $m/z = (M + n)/n$. [c] The differences between the observed and calculated masses of daughter ions. [d] Nomenclature refers to NH_2- and COOH-terminal cleavage fragments according to Roepstorff and Fohlman *(35)* and Biemann *(36, 37)*. Using the same nomenclature, the prime-labeled cleavage fragments are predicted to arise from the second NH_2-terminus of the branched anchor structure. [e] A = H_6EASLPTT.

the endolysin-digested cell walls (Figure 3A). This result further corroborated the previous observation that InlA-MH_6-Cws is anchored to the cell wall compartment *(21)*.

InlA-MH_6-Cws, but not wild-type InlA, contained the H_6 affinity tag for Ni−NTA. Load and eluate fractions of affinity chromatography samples obtained from strains EGD(InlA) and EGD(pGD21) (InlA and InlA-MH_6-Cws) were subjected to immunoblotting with α-InlA and α-H6 (Figure 3B). α-H6 detected InlA-MH_6-Cws in both the load and eluate fractions of EGD(pGD21). No α-H6 signal was observed in the sample of strain EGD. Immunoblotting of the same samples with α-InlA revealed the presence of InlA in the load but not in the eluate of the strain EGD samples, indicating that our purification scheme selectively purified InlA-MH_6-Cws but not wild-type InlA.

COOH-Terminal Anchor Peptides of InlA-MH_6-Cws. Purified InlA-MH_6-Cws was cleaved at methionine residues with CNBr. Cleavage fragments were subjected to affinity chromatography on Ni−NTA, thereby purifying COOH-terminal anchor peptides carrying the H_6 tag. The affinity chromatography eluate was analyzed by rpHPLC on C18 column, which revealed one major and several minor peaks of absorption at 214 nm (Figure 4A). The major absorption peak at 25% CH_3CN (30 min) was analyzed by Edman degradation, which generated the peptide sequence NH_2-H_6-EASLPTT (Table 1). Cycle 14 and 15 (following the last threonine) did not yield a phenylthiohydantoin modified amino acid, indicating that the threonine of the LPXTG motif was not linked to the remainder of the sorting signal (H_6-EASLPTTDSDNA..). During cycle 1, 194 pmol of phenylthiohydantoin-histidine and 62 pmol of phenylthiohydantoin-alanine were eluted off the sequencer column, suggesting that approximately 28% of the COOH-terminal anchor peptides may represent branched peptides with two NH_2-termini available for Edman degradation (Table 1). The major absorption peak at 25% CH_3CN was analyzed by MALDI-MS and signals at *m/z* 1841, 1912, 2083, 2212, 2283, 2354, 2583, and 2866 were observed (Figure 4B). These measurements cannot be explained as COOH-terminal peptide (NH_2-H_6EASLPTT-COOH, calculated molecular mass 1523.6 Da)

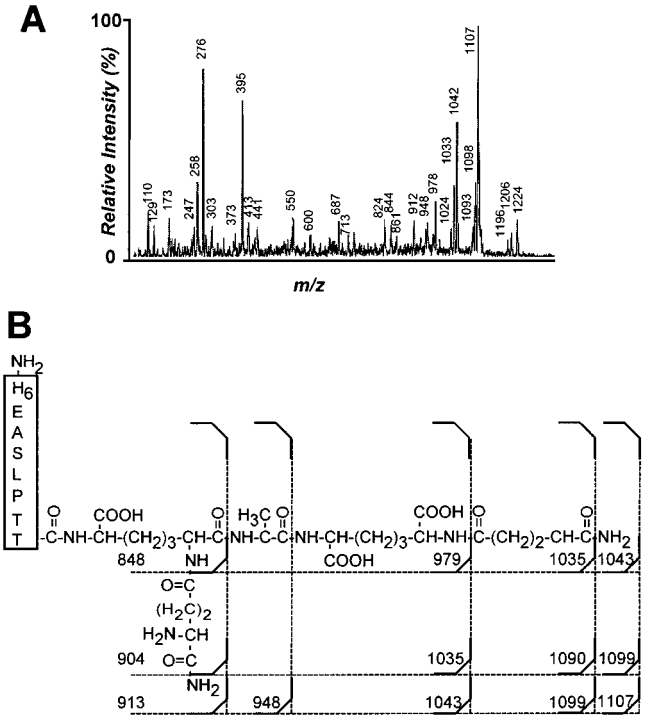

FIGURE 6: Structure of the 2212 Da COOH-terminal InlA-MH_6-Cws anchor peptide from endolysin-digested *L. monocytogenes*. (A) MS/MS analysis of the doubly charged parent ion at *m/z* 1107. (B) CID-generated daughter ions were compared with the structural model. See Table 5 for a complete listing of the observed ions, proposed structures, and calculated masses.

alone but must be accounted for by linked listerial cell wall subunits.

Phage endolysin cuts the amide bond between L-Ala and D-iGln in the listerial cell wall (Figure 1B). If the COOH-terminal threonine of surface protein were linked to the *m*-Dpm side chain (crossbridge) of the listerial cell wall, compounds observed by MALDI-MS may be explained as branched peptides with linked cell wall fragments. This could indeed be accomplished (Table 2). The predominant signal of *m/z* 2212 was explained as singly cross-linked murein tethered to surface protein [D-iGln-*m*-Dpm-(NH_2-H_6EASLPTT-)-D-Ala-*m*-Dpm-(D-iGln)]. The second most abundant signals were interpreted as surface protein linked to murein monomer [*m/z* 1841; D-iGln-*m*-Dpm-(NH_2-H_6EASLPTT-)-D-Ala] or cross-linked dimer [*m/z* 2283; D-iGln-*m*-Dpm-(NH_2-H_6-EASLPTT-)-D-Ala-*m*-Dpm-(D-iGln)-D-Ala]. Some anchor peptides were linked to non-cross-linked peptidoglycan presumably generated from either tripeptide [*m/z* 1841, NH_2-H_6EASLPTT-*m*-Dpm-(iGln)] or tetrapeptide wall fragments [*m/z* 1912, NH_2-H_6EASLPTT-*m*-Dpm-(iGln)-D-Ala]. However, the majority of peptides were attached to 2, 3, and 4 peptidoglycan subunits that were cut at either the L-Ala or the D-iGln moieties. The presence of L-Ala in peptidoglycan linked to anchor peptides explained the appearance of L-Ala during the first Edman degradation cycle. As phage endolysin is not known to cleave at this site *(18, 26)*, we think it is likely that these wall peptide fragments may be generated by endogenous *N*-acetylmuramoyl-L-Ala-amidase activity of *L. monocytogenes* EGD *(27)*.

Fraction 33 (28% CH_3CN) of the rpHPLC chromatogram, encompassing the second largest peak of absorption at 214 nm, was also analyzed by MALDI-MS (Figure 4C), which revealed signals at *m/z* 2939, 3182, 3311, 3386, 3684, and 3754. These signals were explained as surface protein tethered to the *m*-Dpm of multiply cross-linked peptidoglycan (Table 3). Thus, although the rpHPLC chromatogram failed to fully resolve COOH-terminal anchor peptides with small mass differences, separation of other anchor species with larger mass increments was achieved.

Structure of Anchor Peptides of 1841 and 2212 Da. To determine the nature of the linkage between surface proteins and the cell wall of listeria, we subjected the sample of fraction 30 to ESI-MS. The compound of 1841 Da, generating the doubly charged parent ion with *m/z* 921.5, was analyzed in an MS/MS experiment (Figure 5). The spectrum

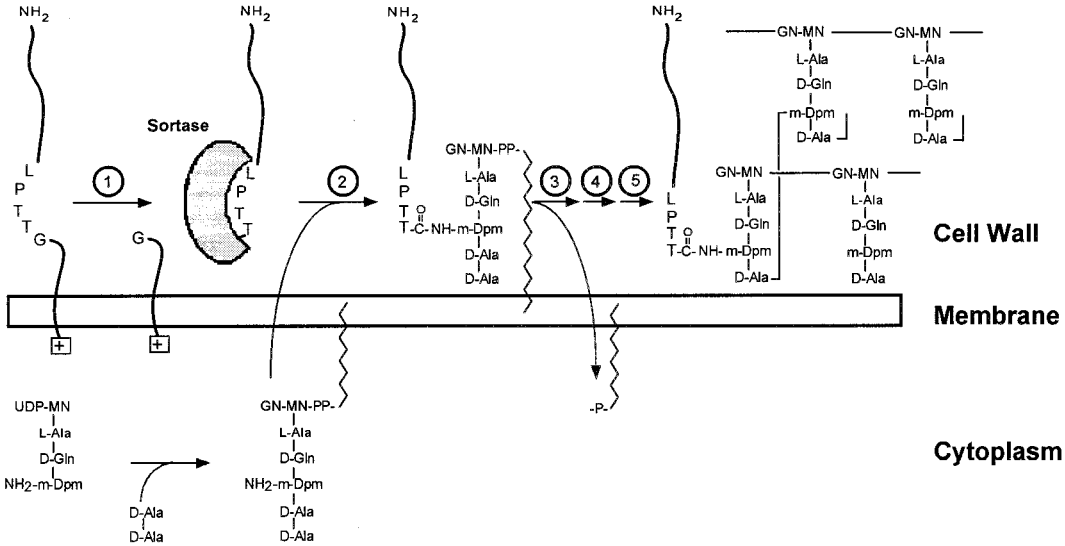

FIGURE 7: Model for the sorting of surface proteins to the cell wall of *L. monocytogenes* modified after Ton-That et al. *(7)*. Peptidoglycan precursor molecules are synthesized in the bacterial cytoplasm and translocated across the membrane. Surface proteins are first cleaved (1) between the threonine (T) and the glycine (G) of the LPXTG motif and subsequently linked to the peptidoglycan precursor molecule (2). The proposed intermediate of surface protein linked to peptidoglycan precursor may then be incorporated into the cell wall by transglycosylase (3) and transpeptidation reactions (4). Carboxypeptidase (5) may cleave the D-Ala-D-Ala of some cell wall pentapeptides to yield un-cross-linked tetrapeptides.

Table 5: Summary of CID Daughter Ions Produced during MS/MS of the Endolysin-Released Anchor Peptide with *m/z* 2212 and Their Proposed Structural Assignments (Figure 5)

observed *m/z*[a]	charge state	calculated *m/z*[b]	Δobs − calc[c]	proposed structure	ion type[d]
110.3	+1	110.1	+0.2	H	a_1
138.5	+1	138.1	+0.4	H	b_1
69.5	+2	69.6	−0.1	H	b_1
247.4	+1	247.3	+0.1	HH	a_2
258.2	+1	257.3	+0.9	HH (−H_2O)	b_2
275.6	+1	275.3	+0.3	HH	b_2
138.5	+2	138.1	+0.4	HH	b_2
413.0	+1	412.4	+0.6	HHH	b_3
395.0	+1	394.4	+0.6	HHH (−H_2O)	b_3
549.5	+1	549.6	−0.1	HHHH	b_4
275.6	+2	275.3	+0.3	HHHH	b_4
282.8	+2	282.8	0.0	HHHH	c_4
657.8	+1	658.7	−0.9	HHHHH	a_5
687.2	+1	686.7	+0.5	HHHHH	b_5
823.7	+1	823.8	−0.1	HHHHHH	b_6
413.0	+2	412.4	+0.6	HHHHHH	b_6
952.1	+1	953.0	−0.9	H_6E	b_7
1023.9	+1	1024.1	−0.2	H_6EA	b_8
1092.5	+1	1093.1	−0.6	H_6EAS (−H_2O)	b_9
1112.0	+1	1111.1	+0.9	H_6EAS	b_9
1195.7	+1	1196.3	−0.6	H_6EAS	a_{10}
600.2	+2	598.6	+1.6	H_6EASL	a_{10}
1223.9	+1	1224.7	−0.8	H_6EASL	b_{10}
613.4	+2	612.6	+0.8	H_6EASL	b_{10}
1205.9	+1	1206.3	−0.4	H_6EASL (−H_2O)	b_{10}
440.6	+2	441.5	−0.9	HHHEASLP	a_{11}, y_{13}[e]
661.7	+2	661.2	+0.5	H_6EASLP	b_{11}
697.7	+2	697.8	−0.1	H_6EASLPT	a_{12}
713.3	+2	711.8	+1.5	H_6EASLPT	b_{12}
761.6	+2	762.3	−0.7	H_6EASLPTT	b_{13}
847.7	+2	847.9	−0.2	A-*m*-Dpm[f]	b_{14}, y_1'' [e]
843.5	+1	843.9	−0.4	PTT-*m*-Dpm-(D-iGln)-D-Ala-*m*-Dpm (−H_2O)	y_6, y_1'/y_1'' [e]
860.9	+1	861.9	−1.0	PTT-*m*-Dpm-(D-iGln)-D-Ala-*m*-Dpm	y_6, y_1'/y_1'' [e]
912.4	+2	912.5	−0.1	D-iGln-*m*-Dpm-(A)	b_{14}
904.4	+2	904.0	−0.1	D-iGln-*m*-Dpm-(A) (−NH_2)	b_{14}
947.5	+2	948.0	−0.5	D-iGln-*m*-Dpm-(A)-D-Ala	b_{15}
978.2	+2	979.0	−0.8	*m*-Dpm-(A)-D-Ala-*m*-Dpm	y_1', y_1'' [e]
1033.1	+2	1034.6	−1.5	*m*-Dpm-(A)-D-Ala-*m*-Dpm-(D-iGln) (−NH_2)	y_1''/y_1' [e]
1042.2	+2	1043.1	−0.9	*m*-Dpm-(A)-D-Ala-*m*-Dpm-(D-iGln)	y_1''/y_1' [e]
1092.5	+2	1090.2	+2.3	D-iGln-*m*-Dpm-(A)-D-Ala-*m*-Dpm-(D-iGln)(−2NH_2)	
1097.9	+2	1098.7	−0.8	D-iGln-*m*-Dpm-(A)-D-Ala-*m*-Dpm-(D-iGln) (−NH_2)	
128.6	+2	129.1	−0.5	D-iGln	b_1'/b_1'' [e]
173.3	+1	173.2	+0.1	*m*-Dpm (−H_2O)	y_1, y_1' [e]
191.6	+1	191.2	+0.4	*m*-Dpm	y_1, y_1' [e]
302.6	+1	301.3	+1.3	*m*-Dpm-(D-iGln) (−H_2O)	y_1
318.8	+1	319.3	−0.5	*m*-Dpm-(D-iGln)	y_1
373.1	+1	372.4	+0.7	D-Ala-*m*-Dpm-(D-iGln) (−H_2O)	y_2
1106.6	+2	1107.1	−0.5	D-iGln-*m*-Dpm-(A)-D-Ala-*m*-Dpm-(D-iGln)	parent ion

[a] See Figure 5A for relative intensity of daughter ions. [b] Calculations are based on average masses; for n protonated species the formula is $m/z = (M + n)/n$. [c] Differences between the observed and calculated masses of daughter ions. [d] Nomenclature refers to NH_2- and COOH−terminal cleavage fragments according to Roepstorff and Fohlman *(35)* and Biemann *(36, 37)*. Using the same nomenclature, the prime-labeled cleavage fragments are predicted to arise from the second NH_2-terminus of the branched anchor structure. [e] Fragments thought to arise by two cleavages. [f] A = H_6EASLPTT.

of daughter ion fragments generated by CID is listed in Table 4. The presence of the ions with *m/z* 761 (+2) and 857 (+2) revealed the linkage between the carboxyl of threonine and the γ-amino group of *m*-Dpm. The fact that this bond cannot be hydrolyzed by Edman degradation further corroborates the notion that the side-chain γ-amino group of *m*-Dpm must be involved in surface protein anchoring. We also investigated the structure of the anchor peptide tethered to murein dimer (2212 Da) (Figure 6). MS/MS analysis of the doubly charged parent ion at *m/z* 1107 generated a spectrum of daughter ion fragments, which are listed in Table 5. Daughter ions with *m/z* 847.7 (+2) and 978.2 (+2) revealed the linkage between the carboxyl of threonine and the γ-amino group of *m*-Dpm as well as the amide bond between D-Ala and *m*-Dpm of the two cross-linked peptidoglycan subunits. Thus, data obtained with MALDI-MS, MS/MS, and Edman degradation experiments are consistent with the amide linkage between the COOH-terminal threonine of surface protein and the γ-amino group of *m*-Dpm within cross-linked peptidoglycan.

DISCUSSION

Gram-positive bacteria display a variety of proteins on the cell surface that are thought to play important roles during the pathogenesis of human infections *(1, 28, 29)*. For example, internalin A, and perhaps other members of the *L. monocytogenes* internalin family, cause bacterial invasion into certain human epithelial cells by binding to the E-cadherin receptor on the surface of host cells *(19, 30, 31)*. Receptor recognition appears to be a key event during the pathogenesis of listeria infections as the spectrum of potential hosts is limited by the species-specific interaction between E-cadherin and internalin A *(32)*. Thus, methods that interfere with surface protein display and receptor interaction may

be used as an antiinfective therapy to either prevent or cure human infections with Gram-positive bacteria.

Many Gram-positive surface proteins are thought to be covalently linked to the bacterial cell wall by a mechanism requiring a COOH-terminal sorting signal with a conserved LPXTG motif *(1)*. While the nature of the linkage between surface proteins and the cell wall of *S. aureus* has been known for some time, the generality of these findings has thus far not been established *(6)*. By examining the cell wall anchor structure of internalin A in listeria, we show here that the COOH-terminal threonine of surface protein is linked to the *m*-Dpm of cell wall peptides (Figure 7). Thus, the sorting signal of internalin, similar to that of staphylococcal protein A, is cleaved between the threonine and the glycine of the LPXTG motif. Furthermore, the amide linkage between the carboxyl of threonine and the γ-amino group of *m*-Dpm reveals that internalin is also tethered to the peptidoglycan crossbridge. These results strongly suggest that the amide bond exchange mechanism of the sorting hypothesis is universal in Gram-positive bacteria *(6)*. The generality of the sorting hypothesis is also supported by the fact that the sortase gene is conserved in sequence and has been found in the genomes of all Gram-positive bacteria that have been sequenced to date *(10)*. Hence, compounds that interfere with surface protein anchoring in staphylococci may also prevent anchoring of listerial internalin A or any other Gram-positive surface protein.

While the LPXTG motif and the free amino of peptidoglycan crossbridges are conserved in Gram-positive bacteria *(1)*, the overall chemical structure of crossbridges is not *(33)*. In staphylococci, the crossbridge is composed of five glycines, whereas in many streptococcal species it consists of two alanines *(15)*. How can sortase be conserved in sequence and presumably in function if the chemical nature of its substrate, the peptidoglycan crossbridge, is variable? This question has been previously addressed and staphylococcal mutants that synthesize altered crossbridges containing serine residues or three or one glycine residues were still able to anchor surface proteins *(34)*. Perhaps sortase recognizes the peptidoglycan substrate by a feature other than the crossbridge. Recent work suggested that the lipid II precursor and not the mature assembled cell wall may serve as a substrate for the sorting reaction *(11)*. While this hypothesis remains to be formally proven and awaits the purification and characterization of a lipid-linked surface protein intermediate, it is conceivable that features such as undecaprenol pyrophosphate or the conserved sequence of the cell wall stem-peptide are recognized by sortase.

ACKNOWLEDGMENT

We thank Dr. P. Cossart, Dr. D. Portnoy, and Dr. J. F. Miller for the gift of *L. monocytogenes* strain EGD and antisera against InlA and ActA. We also thank Dr. R. Stevens for help with the MALDI-MS measurements and Dr. W. W. Navarre and H. Ton-That for instruction as well as critical reading of the manuscript.

REFERENCES

1. Navarre, W. W., and Schneewind, O. (1999) *Microbiol. Mol. Biol. Rev. 63*, 174−229.
2. Schneewind, O., Model, P., and Fischetti, V. A. (1992) *Cell 70*, 267−281.
3. Schneewind, O., Mihaylova-Petkov, D., and Model, P. (1993) *EMBO 12*, 4803−4811.
4. Navarre, W. W., and Schneewind, O. (1996) *J. Bacteriol. 178*, 441−446.
5. Navarre, W. W., and Schneewind, O. (1994) *Mol. Microbiol. 14*, 115−121.
6. Schneewind, O., Fowler, A., and Faull, K. F. (1995) *Science 268*, 103−106.
7. Ton-That, H., Faull, K. F., and Schneewind, O. (1997) *J. Biol. Chem. 272*, 22285−22292.
8. Navarre, W. W., Ton-That, H., Faull, K. F., and Schneewind, O. (1998) *J. Biol. Chem. 273*, 29135−29142.
9. Navarre, W. W., Ton-That, H., Faull, K. F., and Schneewind, O. (1999) *J. Biol. Chem. 274*, 15847−15856.
10. Mazmanian, S., Liu, G., Ton-That, H., and Schneewind, O. (1999) *Science 285*, 760−765.
11. Ton-That, H., and Schneewind, O. (1999) *J. Biol. Chem. 274*, 24316−24320.
12. Matsuhashi, M., Dietrich, C. P., and Strominger, J. L. (1965) *Proc. Natl. Acad. Sci. U.S.A. 54*, 587−594.
13. Strominger, J. L., Izaki, K., Matsuhashi, M., and Tipper, D. J. (1967) *Fed. Proc. 26*, 9−18.
14. Ton-That, H., Liu, G., Mazmanian, S. K., Faull, K. F., and Schneewind, O. (2000) *Proc. Natl. Acad. Sci. U.S.A. 96*, 12424−12429.
15. Schleifer, K. H., and Kandler, O. (1972) *Bacteriol. Rev. 36*, 407−477.
16. Kamisango, K.-I., Saiki, I., Tanio, Y., Okumura, H., Araki, Y., Sekikawa, I., Azuma, I., and Yamamura, Y. (1982) *J. Biochem. (Tokyo) 92*, 23−33.
17. Saiki, I., Kamisango, K.-I., Tanio, Y., Okumura, H., Yamamura, Y., and Azuma, I. (1982) *Infect. Immun. 38*, 58−66.
18. Loessner, M. J., Schneider, A., and Scherer, A. (1996) *Appl. Environ. Microbiol. 62*, 3057−3060.
19. Gaillard, J.-L., Berche, P., Frehel, C., Gouin, E., and Cossart, P. (1991) *Cell 65*, 1127−1141.
20. Dramsi, S., Dehoux, P., and Cossart, P. (1993) *Mol. Microbiol. 9*, 1119−1122.
21. Lebrun, M., Mengaud, J., Ohayon, H., Nato, F., and Cossart, P. (1996) *Mol. Microbiol. 21*, 579−592.
22. Cossart, P. (1994) *Methods Enzymol. 236*, 551−563.
23. Sheehan, B., Klarsfeld, A., Msadek, T., and Cossart, P. (1995) *J. Bacteriol. 177*, 6469−6476.
24. Kocks, C., Gouin, E., Tabouret, M., Berche, P., Ohayon, H., and Cossart, P. (1992) *Cell 68*, 521−531.
25. Sokolovic, Z., Jutta, R., Wuenscher, M., and Goebel, W. (1993) *Mol. Microbiol. 8*, 219−227.
26. Loessner, M. J., Wendlinger, G., and Scherer, S. (1995) *Mol. Microbiol. 16*, 1231−1241.
27. McLaughlan, A. M., and Foster, S. J. (1998) *Microbiol. 144*, 1359−1367.
28. Patti, J. M., Allen, B. L., McGavin, M. J., and Höök, M. (1994) *Annu. Rev. Microbiol. 48*, 89−115.
29. Ireton, K., and Cossart, P. (1997) *Annu. Rev. Genet. 31*, 113−138.
30. Dramsi, S., Dehoux, P., Lebrun, M., Goossens, P., and Cossart, P. (1995) *Infect. Immun. 65*, 1615−1625.
31. Mengaud, J., Ohayon, H., Gounon, P., Mege, M., and Cossart, P. (1996) *Cell 84*, 923−932.
32. Lecuit, M., Dramsi, S., Gottardi, C., Fedor-Chaiken, M., Gumbiner, B., and Cossart, P. (1999) *EMBO J. 18*, 3956−3963.
33. Ghuysen, J.-M. (1968) *Bacteriol. Rev. 32*, 425−464.
34. Ton-That, H., Labischinski, H., Berger-Bächi, B., and Schneewind, O. (1998) *J. Biol. Chem. 273*, 29143−29149.
35. Roepstorff, P., and Fohlman, J. (1984) *Biomed. Mass Spectrom. 11*, 601.
36. Biemann, K. (1988) *Biomed. Environ. Mass Spectrom. 16*, 99−111.
37. Biemann, K. (1992) *Annu. Rev. Biochem. 61*, 977−1010.

BI992347O